Catal Lett
DOI 10.1007/s10562-016-1948-6

A Novel Consecutive Approach for the Preparation of Cu–MgO Catalysts with High Activity for Hydrogenation of Furfural to Furfuryl Alcohol

Mohammad Ghashghaee[1,2] · Samahe Sadjadi[2,3] · Samira Shirvani[1,2] · Vahid Farzaneh[1,2]

Received: 17 September 2016 / Accepted: 6 December 2016

Abstract A consecutive approach is introduced and tested for the first time to synthesize copper-magnesia catalysts with different (Cr, Ca, and Co) promoters for the catalytic hydrogenation of furfural. The comparison of the activity of these catalysts with that prepared via conventional co-precipitation indicated the superior activity of the former. A stable conversion of furfural (up to 91%) to furfuryl alcohol was achieved over the thus-prepared Cu–MgO and CaCu–MgO catalysts. However, both CoCu–MgO and CaCu–MgO demonstrated higher selectivities (about 99%) than the other two samples (Cu–MgO and CrCu–MgO). No direct interconnection was established between the catalytic activity and structural features of the catalysts, however.

Graphical Abstract

Keywords Hydrogenation · Furfuryl alcohol · Furfural · Copper catalysts · Hydrothermal synthesis.

1 Introduction

Energy security issues, environmental concerns such as the increase in the green house gases and consequently global warming [1] together with the depletion of the crude reserves [2–4] have led to increasing the use of low-carbon biofuels derived from lignocellulosic or oleochemical biomass sources as alternatives to fossil fuels [5–10].

Furfural is among the most promising biomass-derived molecules, which can be potentially used for the synthesis of a broad range of value-added chemicals such as furoic acid, 2-methylfuran, furfurylamine, maleic acid, furan, linear alkanes, 1,5-pentanediol, cyclopentanone, 2-methyl tetrahydrofuran, furfuryl alcohol and fuels [8, 11–18]. Among the chemical transformations of furfural, catalytic hydrogenation of furfural which can be achieved in liquid [13, 19–21] or gas [10, 22, 23] phases in the presence of

✉ Mohammad Ghashghaee
m.ghashghaee@ippi.ac.ir

1 Faculty of Petrochemicals, Iran Polymer and Petrochemical Institute, P.O. Box 14975-112, Tehran, Iran

2 Biomass Conversion Science and Technology (BCST) Division, Iran Polymer and Petrochemical Institute, P.O. Box 14975-115, Tehran, Iran

3 Gas Conversion Department, Faculty of Petrochemicals, Iran Polymer and Petrochemical Institute, P.O. Box 14975-112, Tehran, Iran

metal-based catalysts is of particular importance [8]. The utility of furfuryl alcohol for the production of adhesives, furan fiber-reinforced plastics, thermostatic resins, liquid resins, foundry resins, farm chemicals, lubricants, dispersing agents, ascorbic acid, and lysine has been proven [22, 24–26].

Industrially, the gas-phase hydrogenation of furfural is accomplished at temperatures ranging between 403 and 473 K and pressures up to 30 bar under commercial copper chromate catalysts [9, 27]. Copper chromate can result in selective formation of furfuryl alcohol. However, this catalyst is toxic and exhibited moderate activity. To furnish a solution to these problems many attempts have been devoted to develop alternative Cr-free catalysts. To date, various mono metallic and bimetallic catalysts including Cu, Ni, Pd, Co, Ru, Ir, and Pt supported on a relatively inert material such as silica and alumina have been prepared [16, 28–32] among which Cu-based catalysts, especially Cu-MgO has gained increasing attention because of its low cost, high activity and selectivity to furfuryl alcohol [17, 22, 28, 33–36].

Herein, we wish to present a novel procedure based on a combination of co-precipitation and hydrothermal methods for the preparation of a series of Cu–MgO catalysts with various promoters (Co, Ca, and Cr) and definite morphologies. The main reason for using the promoters and developing the multimetallic catalysts was taking advantages of the multicomponent catalyst systems compared to monometallic counterparts and consequently improving the catalytic performance of the catalyst. Cr is a promoter widely used for improving the catalytic performance of the Cu–MgO catalysts [37–39]. It is even used in the commercialized catalyst used for industrial conversion of furfural to furfuryl alcohol. Ca is a basic promoter which in proper amount can improve the stability of the Cu-based hydrogenation catalysts [40]. According to previous reports, Co promoter can increase the selectivity of the process by reducing the unwanted by-products [41]. Therefore, these three promoters were chosen for possible effects on the base catalyst.

The catalytic activities of these catalysts as well as the effects of the promoters on the catalytic performances are studied for the gas-phase hydrogenation of furfural to furfuryl alcohol. Moreover, the catalytic activities of Cu-MgO catalysts prepared via the new consecutive approach and the classic co-precipitation method are compared.

2 Experimental

2.1 Materials

All chemicals applied for the catalysts preparation were used directly without any further purification after the purchase. $Mg(NO_3)_2{\cdot}6H_2O$ (ACS reagent, 99%), $Cu(NO_3)_2{\cdot}3H_2O$ (99.5%), K_2CO_3 (ACS reagent, 99.5%), $Ca(NO_3)_2{\cdot}4H_2O$ (99%) and $Co(NO_3)_2{\cdot}6H_2O$ (99%) were provided from Merck. $Cr(NO_3)_3{\cdot}9H_2O$ (97%) was purchased from Scharlau. The material employed for the studying the catalytic activity included furfural (98.90%, Merck) and high purity hydrogen (99.99%) and nitrogen (99.99%).

2.2 Catalyst Preparation Using Co-Precipitation Method

A catalyst sample, which is referred to as CM0, was prepared by conventional co-precipitation method. Briefly, 1 M solution of K_2CO_3 was added to a mixture of $Cu(NO_3)_2{\cdot}3H_2O$ (1 M) and $Mg(NO_3)_2{\cdot}6H_2O$ drop wisely to form precipitate at a pH of 9.0. The resulting solution was stirred vigorously for 3 h. Upon completion, the precipitate was filtered and washed with distilled water and dried at 393 K for 15 h. The final catalyst was obtained by calcination in air at 723 K for 5 h with the heating rate of 1 K/min.

2.3 Catalyst Preparation Using Consecutive Approach

The catalysts were prepared by a novel consecutive procedure based on a combination of co-precipitation and hydrothermal methods. The typical procedure includes precipitation of a mixture of 1 M solution of $Cu(NO_3)_2{\cdot}3H_2O$ and $Mg(NO_3)_2{\cdot}6H_2O$ with the percentage weight ratio of 16:84 for Cu:MgO by drop wise addition of 1 M aqueous solution of K_2CO_3 at room temperature at a pH of 9.0 followed by stirring for 3 h. Subsequently, the mixture was transferred to a Teflon-lined autoclave and subjected to hydrothermal treatment for 24 h at 200 °C. The precipitate was filtered and washed with distilled water. The final catalyst, named as CM1, was obtained by drying the precipitate at 423 K for 15 h and calcination in air at 723 K for 5 h with the heating rate of 1 K/min. Three other catalysts were also prepared according to the above-mentioned procedure for CM1 except that three different promoters (P) including $Cr(NO_3)_3{\cdot}9H_2O$, $Ca(NO_3)_2{\cdot}4H_2O$ and $Co(NO_3)_2{\cdot}6H_2O$ with percentage weight ratio of 1:15:84 for P:Cu:MgO were used. The catalysts were denoted as CM2, CM3 and CM4, respectively.

2.4 Catalyst and Products Characterization

To characterize the novel catalysts, BET, SEM/EDX, and XRD techniques were used along with TGA of the spent catalysts. BET analyses were carried out via nitrogen physisorption using a Quantachrome Chembet 3000 sorption analyzer at 77 K. Prior to analysis, the samples were degassed at 393 K for 3 h. SEM/EDX analyses of all catalysts were performed by a Tescan instrument, using

Au-coated samples with an acceleration voltage of 20 kV. Room temperature powder X-ray diffraction patterns were collected using a Siemens, D5000. Cobalt Co Kα radiation was used from a sealed tube. Data were collected in the 2θ range of 25–80° with a step size of 0.02° and an exposure time of 2 s per step. The TGA spectra were obtained using a Perkin Elmer Pyris 1 apparatus with 10 °C/min ramping in air. The product samples were collected in an ice-bath condenser and taken every few minutes for analysis on a gas chromatograph (GC) equipped with a capillary column and a flame ionization detector (FID). The standard designation of the peaks was made by calibration on an Agilent 6890 series GC system equipped with an Agilent 5973 network mass selective detector (MSD). The instrument contained an HP-5ms column of 30 m × 0.25 mm ID and 0.25 μm film thickness.

2.5 Catalyst Activity

The catalytic activity of the catalysts for the hydrogenation of furfural (FF) was evaluated in a tubular reactor of 10 mm internal diameter. The catalyst (0.7 g) was initially reduced in hydrogen flow diluted in nitrogen with the total flow rate of ~6 l/(g h) at 523 K for 3 h and then was cooled down to the reaction temperature of 453 K in pure hydrogen flow. After that, the feedstock was injected into the reactor with a space velocity (WHSV) of 1.7 g/(g h). The reactions were implemented under atmospheric conditions with an H_2/FF volumetric ratio of 10 for 4 h. The reaction products were analyzed by GC-MS which was equipped with an FID and a capillary column.

3 Result and Discussion

To figure out the influence of hydrothermal treatment, the copper-magnesia catalysts synthesized via the conventional co-precipitation (CM0) and the new consecutive method (CM1) were evaluated for the selective hydrogenation of FF to furfuryl alcohol (FFA), the key green building block for the furan resins. Figure 1 illustrates the activity results of the two catalysts at two times-on-stream of 60 and 600 min. As evident, the Cu-MgO catalyst prepared via the new procedure (CM1) was markedly superior compared to the conventionally synthesized sample (CM0). Although the FFA selectivity with CM0 was striving at the initial time of operation, it reduced drastically over the run length and the FFA yield was too small due to the low conversion levels compared to CM1.

Further, catalytic experiments were also conducted to probe the additional role of Cr, Ca, and Co modifiers on the performance of the mother catalyst. Figure 2 depicts the key performance data from the hydrogenation

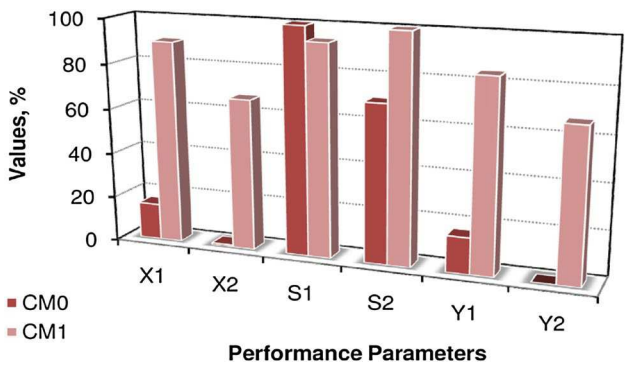

Fig. 1 The performance measures of the Cu–MgO catalysts prepared through conventional co-precipitation and the new combined method for the conversion of FF to FFA at 453 K, 1 atm, WHSV of 1.7 1/h, and H_2/FF of 10 (Symbols X, S, and Y represent conversion, selectivity and yield and the numbers 1 and 2 show the results after 60 and 600 min of operation, respectively). The data were reproducible to within ±2%

experiments at different times on stream. Overall, the feed conversion ranged from ~16 to ~91% over the whole period of operation (~600 min) while the main product (FFA) selectivity remained above 87% at most of the times for all of the catalysts (Fig. 2). The conversion level and correspondingly the yield of FFA followed the order of CM2 < CM4 < CM3 < CM1 as averaged over the whole range of time-on-stream. The initial selectivity to FFA changed in the order of CM3 < CM2 < CM1 < CM4 while the sequence slightly shifted to CM2 < CM1 < CM4 < CM3 at the final times. As indicated from Fig. 2, both the parent (CM1) and the calcium-doped (CM3) catalysts demonstrated better durabilities compared to the Cr-doped (CM2) and Co-promoted (CM4) samples (Fig. 2). Moreover, the parent Cu-MgO catalyst (CM1) demonstrated a mild evolution in its selectivity to FFA with time, whereas the rest of the catalysts (CM2–CM4) showed an almost sustained selectivity over an about 9 h of operation and the selectivity of CM4 demonstrated no abrupt increase from the beginning. While the FFA yield of CM3 passed through a primary maximum of ~85%, the other samples gave descending trends for the yield of FFA with time.

When the productivity of the catalyst is concerned, the original Cu–MgO catalyst (CM1) and the Ca-promoted sample (CM3) were superior in terms of a relatively stable conversion of furfural to furfuryl alcohol such that CM1 produced more FFA than CM3. On the other hand, the CoCu–MgO catalyst (CM4) and the CaCu–MgO sample (CM3) could be chosen if selectivity to FFA mattered most. Among the four catalysts, the CrCu–MgO sample might be regarded as the poorest.

Figure 3 depicts the averaged selectivities of the major byproducts obtained during the reactions on the four catalysts investigated. As indicated from this chart, the

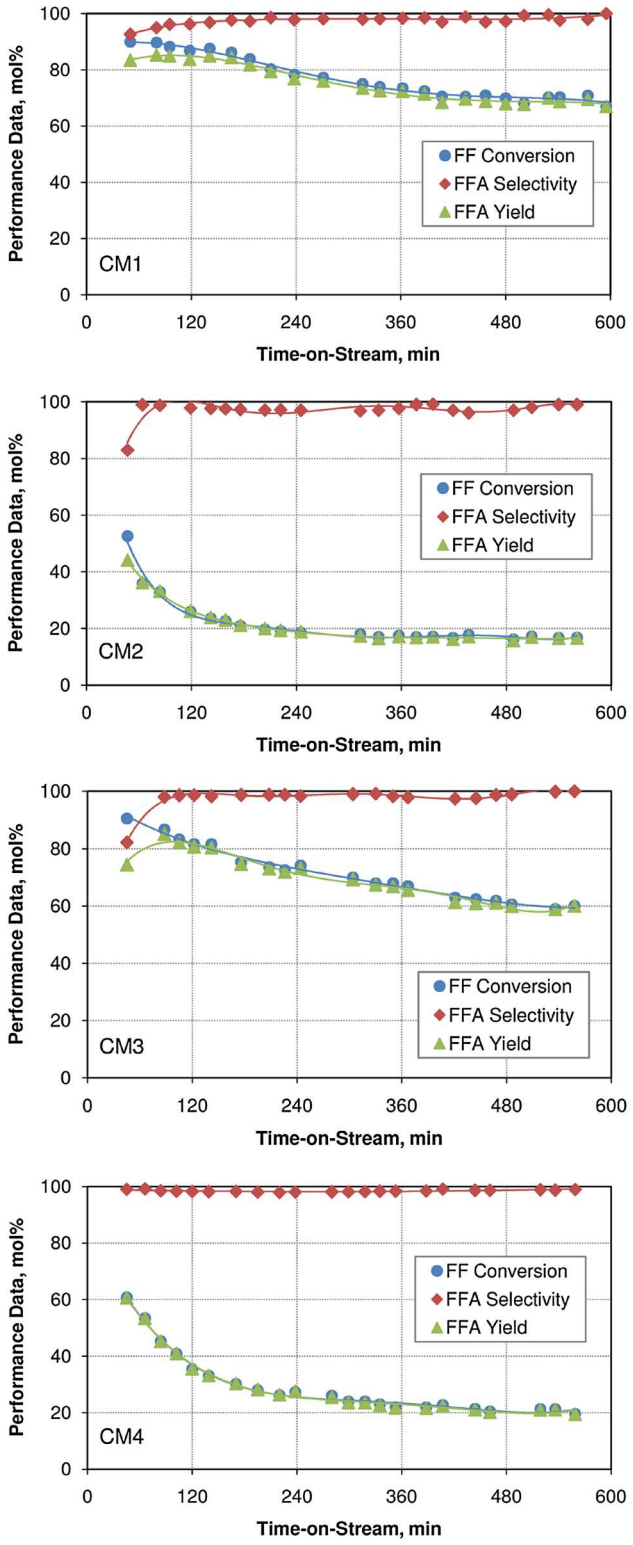

Fig. 2 The conversion, selectivity, and yield of the synthesized copper catalysts with time-on-stream in hydrogenation of FF to FFA at 453 K, 1 atm, WHSV of 1.7 1/h, and H_2/FF of 10. The data were reproducible to within ±2%

main reaction pathways that reduce the FFA selectivity of CM1 were those leading to tetrahydrofurfuryl alcohol (THFA), difurfuryl ether (FFE), 5-methylfurfural (MFF), and 2-methylfuran (MF) while the main byproducts over CM2 were 2-acetylfuran (AF) and MFF. The predominant byproducts over CM3 were, respectively, MFF, THFA, 5-methylfurfuryl alcohol (MFFA), γ-valerolactone (GVL), and AF and CM4 produced MFF and AF as the main by-products. As such, the major byproducts over the CrCu–MgO and CoCu–MgO catalysts were similar. This suggests possibly that the reaction pathways over these two catalysts have been more or less the same. The production of THFA by Cu–MgO and CaCu–MgO samples can also point to some common routes in the reaction networks over these catalysts. Other significant byproducts included 2-methyltetrahydrofuran (MTHF), 1-pentanol (1POL), 2-pentanol (2POL), and δ-valerolactone (DVL) as is shown in Fig. 3.

As discussed above, the use of different promoters could clearly affect the catalytic behavior in terms of selectivity, conversion and durability. To rationalize the results, all synthesized catalysts were characterized and compared by using SEM/EDX, XRD, BET and elemental mapping techniques. The measurement of BET surface areas of all catalysts (Table 1) as well as the catalyst prepared using co-precipitation method, CM0, demonstrated that among the catalyst prepared by the novel procedure, even low amounts of promoters could significantly alter the surface area. The sample with no promoter, CM1, possessed the lowest surface area, 52 m^2/g, while the application of Cr as a promoter (CM2) led to the catalyst with the highest surface area, 132 m^2/g. Considering the fact that CM2 exhibited the poorest catalytic activity, selectivity and durability while CM1 was the catalyst of choice, it can be concluded that possessing a high BET surface area is not determining for a high catalytic activity. Comparing the catalyst samples of CM1 and CM0 which were prepared through two different methods established that the co-precipitation method led to higher surface area (almost twofold) while hydrothermal treatment reduced remarkably the surface area.

The SEM/EDX and elemental mapping analyses of all catalysts are depicted in Fig. 4. The cubic morphology together with small aggregates can be detected for all catalysts which is clearly distinguished from the aggregate like morphology observed for CM0 sample. However, the SEM images of the samples differ to some extent in terms of the size of cubes, degree of aggregation and packing. In CM1, the close-packed cubes formed compact structure. This observation can justify the low surface area of CM1. In the catalysts containing promoters, the size of cubes are larger and the formation of small aggregates is more obvious. Furthermore, the degree of packing is lower than that of CM1. Among the three catalysts, CM3 which possessed

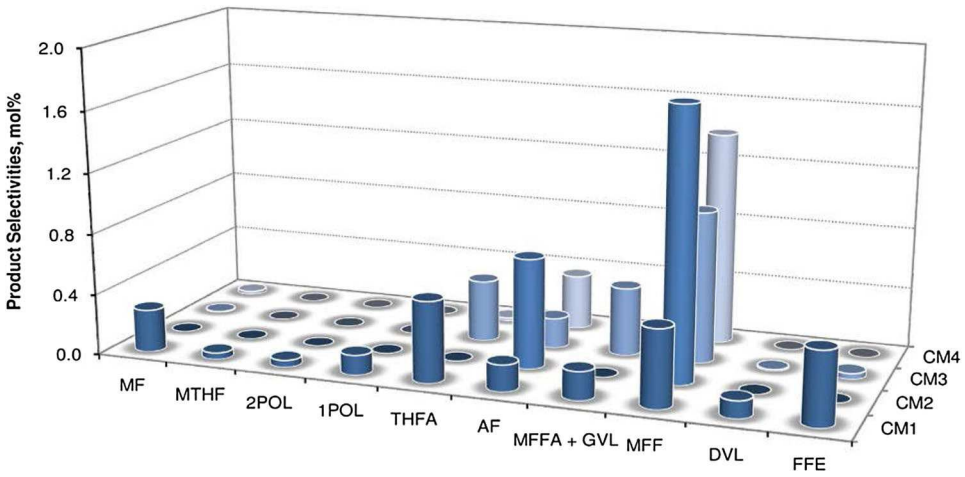

Fig. 3 Average selectivities of byproducts obtained on the four copper-based catalysts over a 600-min period under the reaction conditions of 453 K, 1 atm, WHSV of 1.7 1/h, and H_2/FF of 10

Table 1 Textural properties of the Cu-MgO catalysts

Sample	CuO crystallite size (nm)	Surface area (m^2/g)
CM0	6.2	102
CM1	23.5	52
CM2	23.7	132
CM3	19.2	86
CM4	22.5	125

the second-lowest BET surface area, has the most compact structures.

The EDX analyses (Fig. 5) of the catalysts can confirm the formation of (P)Cu–MgO catalysts. The elemental mapping analyses of samples proved different distributions of catalytic species in the samples. In the cases of CM1, CM2, and CM3, the copper species were well-distributed over the surface of the catalyst. In CM4 sample, however, aggregation of both copper and magnesium species are observed. The low conversion and yield of CM4 can be attributed to the poor distribution of these catalytic species. According to previous reports, the low activity of CM4 can also be attributed to the role of chromium in hampering the reduction of copper oxide species [42]. The elemental mapping analyses of catalysts with promoters, CM2, CM3, and CM4 indicated the uniform distribution of promoter on the surface.

The XRD patterns of all catalysts (Fig. 5) showed the characteristic peaks of MgO (JCPDS card No. 45-0946) and CuO (JCPDS card No. 89-5898 and 45-0937), confirming the formation of the desired catalytic phases. Noteworthy, the XRD patterns of the catalysts containing promoters were similar to those of CM1. According to the previous reports, this observation can be attributed to high dispersion of promoters on the catalyst [43]. The crystallite sizes of CuO were also calculated for all catalysts (Table 2). This value changed in the order of CM0 < CM3 < CM4 < CM1 ≈ CM2. Interestingly, the crystallite sizes of CM1 and CM2, which exhibited the best and the poorest catalytic performance respectively were almost similar. Furthermore, the CM0 sample had the smallest crystallite size. This observation indicated that hydrothermal treatment resulted in increase in the crystallite size. Moreover, no clear connection between the crystallite size as well as catalyst surface area and catalytic activity was observed.

Comparing the catalytic activities of CM0 and CM1 demonstrates that the catalytic activity of CM1, which possesses a lower surface area (almost half the surface area of CM0) and a larger crystallite size (see Table 1), surpassed the activity of CM0. This is against the classic trends usually reported for the activity–surface area relationships. Analogous observations have been reported limitedly in the literature [44]. Therefore, this study clearly established that by changing the synthetic procedure and altering the morphology of the catalysts, the catalytic activity can be tuned. It is suggested that the cubic morphology of the catalyst obtained from the consecutive procedure could provide some specific or more available active sites for the hydrogenation reaction and prevent from the aggregation of the reduced form of the copper species thus improving the activity of the catalyst compared to the sample prepared from the conventional co-precipitation method.

The TGA and DTG curves of the spent catalysts in the temperature range of 25–800 °C are depicted in Fig. 6. The weight loss between 200 and 800 °C was attributed to the coke formed during the hydrogenation of furfural. All of the catalysts mainly showed endotherms in the relatively moderate temperature range of 200–460 °C which can be attributed to the soft coke [45]. As evident, the spent CM2 sample demonstrated the hardest and highest carbonaceous deposits. On the other hand, the lowest oxidation peak

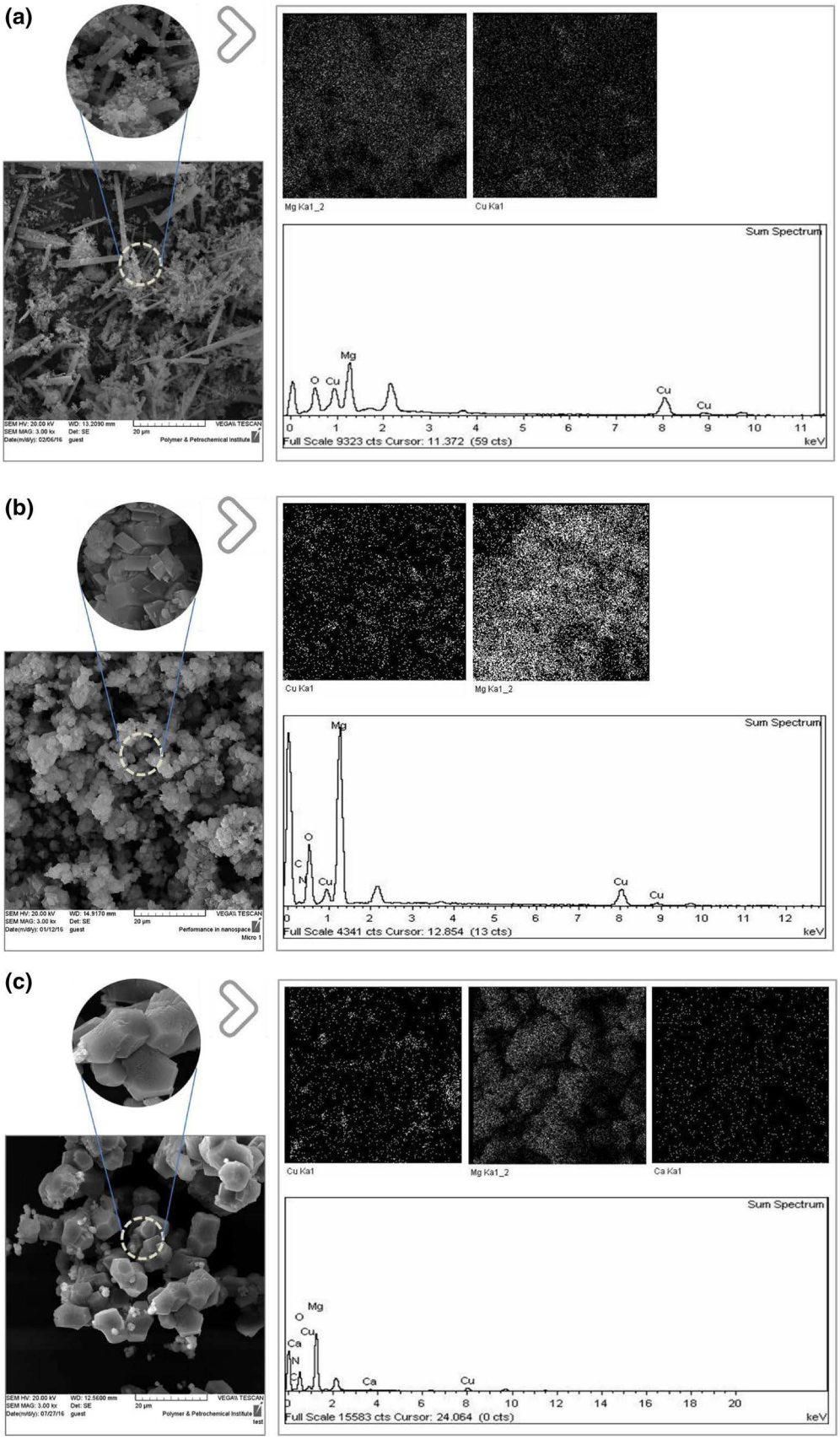

Fig. 4 SEM/EDX and elemental mapping analyses of the five synthesized catalysts. **a** CM0, **b** CM1, **c** CM2, **d** CM3, and **e** CM4

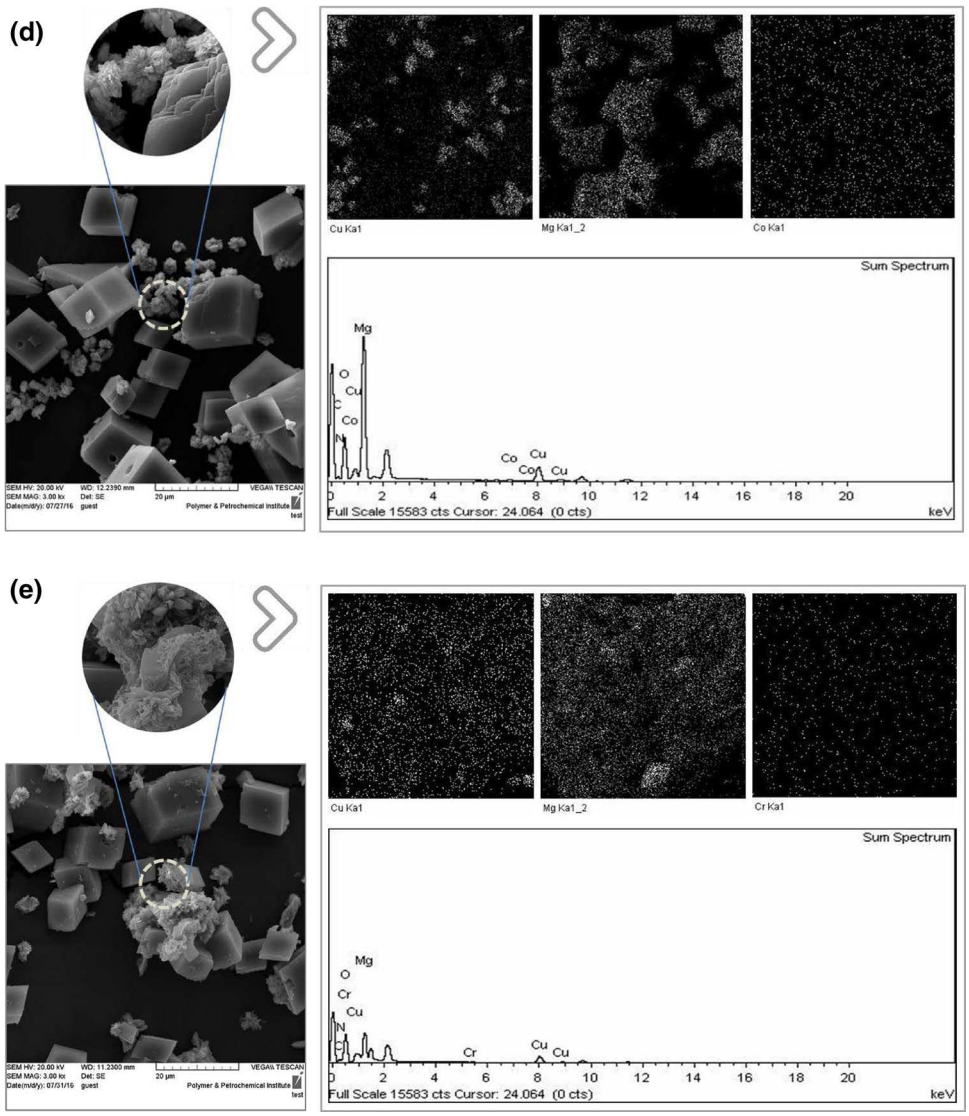

Fig. 4 (continued)

with the lowest amount of coke was obtained for the spent CM3. These results are consistent with the activity trends discussed in this paper. Noteworthy, the major weight loss on CM1 occurred below 200 °C, which corresponds to the release of the physisorbed water molecules [22]. This indicates that the spent CM1 catalyst possessed an exposed Cu-MgO surface mostly uncovered by coke which supports the higher durability of this catalyst observed during the activity tests. The possibility for the formation of soft non-polycyclic species via condensation and rearrangement reactions at low temperatures (below 200 °C) cannot be ruled out [45, 46], however. In spite of presenting a very small DTG stage of mass loss at ~730 °C which is attributable to a really rigid form of coke, the spent CM0 catalyst showed a relatively small amount of coke while performing poorly for the vapor-phase hydrogenation of furfural. This indicates that the catalyst did not possess appropriate active

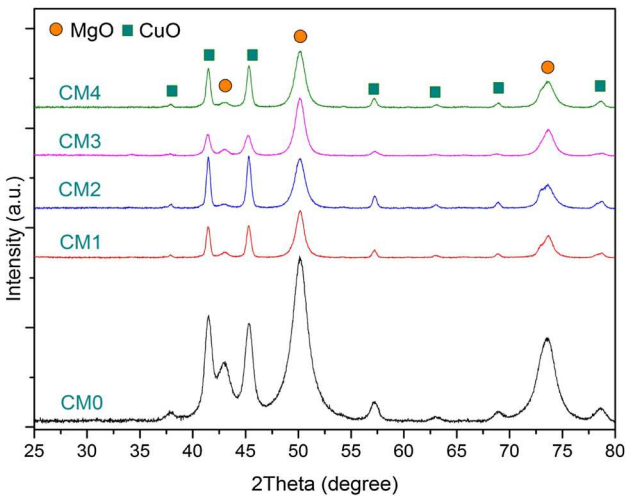

Fig. 5 The XRD patterns of the five synthesized catalysts

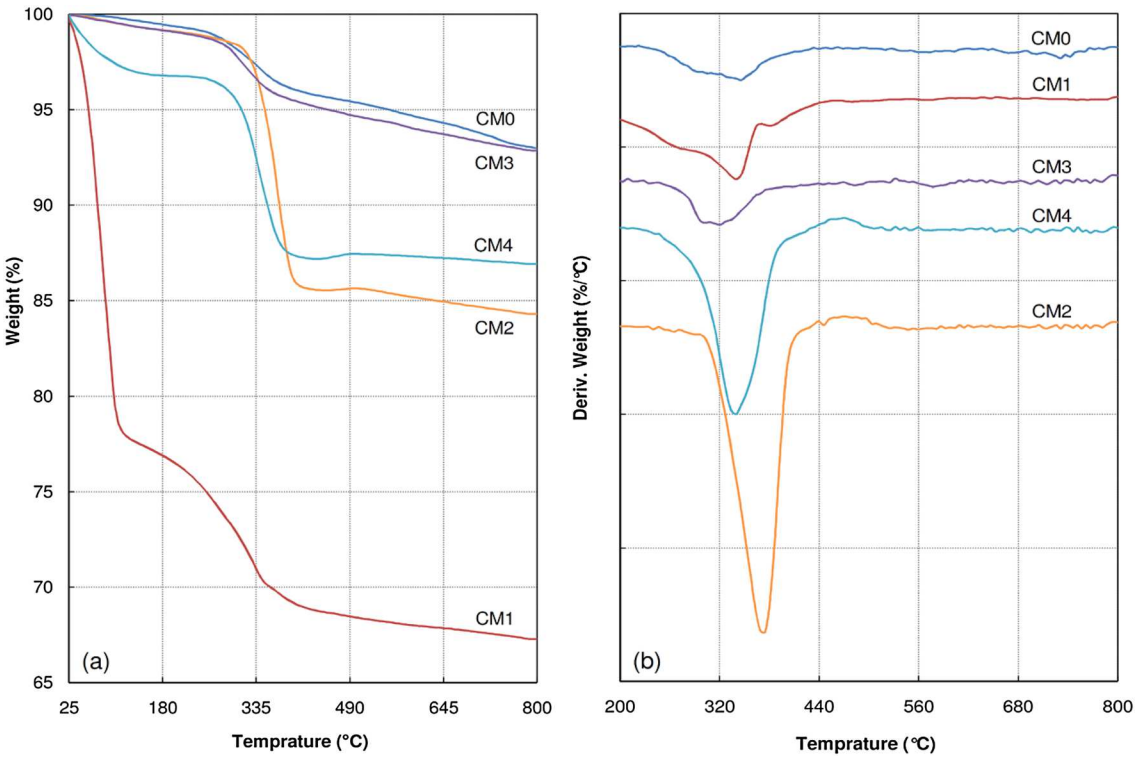

Fig. 6 Thermogravimetric (**a**) and derivative thermogravimetric (**b**) curves of the spent catalysts

sites from the beginning even to trigger the coking reactions. This in turn emphasizes the influence of the preparation method on the appropriate activity of the synthesized catalyst.

3.1 Conclusion

According to the results of structural analyses, it can be concluded that using the initiative consecutive approach leads to the formation of an unprecedented cubic morphology in the Cu–MgO catalyst which can be remarkably influenced by the introduction of promoters. The presence of the promoters can alter the size of cubes and their packing. The higher the packing, the lower the observed BET surface area. A comparison between the results of the new approach and the conventional co-precipitation method indicated the superior performance with the new method. A relatively stable conversion of furfural (91%) to furfuryl alcohol was obtained over the thus-prepared Cu-MgO and CaCu-MgO catalysts. However, CoCu-MgO and CaCu-MgO samples showed higher selectivities (~99%) compared to the other two ones. Interestingly, no distinct relationship could be established between the catalytic activity and structural features of the catalysts.

Acknowledgements The authors appreciate the partial support from Iran Polymer and Petrochemical Institute.

References

1. Halilu A, Ali TH, Atta AY, Sudarsanam P, Bhargava SK, Abd Hamid SB (2016) Highly selective hydrogenation of biomass-derived furfural into furfuryl alcohol using a novel magnetic nanoparticles catalyst. Energy Fuels 30 (3):2216–2226. doi:10.1021/acs.energyfuels.5b02826
2. Zhang X, Tu M, Paice MG (2011) Routes to potential bioproducts from lignocellulosic biomass lignin and hemicelluloses. BioEnergy Res 4 (4):246–257. doi:10.1007/s12155-011-9147-1
3. Dutta S, De S, Saha B, Alam MI (2012) Advances in conversion of hemicellulosic biomass to furfural and upgrading to biofuels. Catal Sci Technol 2 (10):2025–2036. doi:10.1039/c2cy20235b
4. Yu W, Tang Y, Mo L, Chen P, Lou H, Zheng X (2011) One-step hydrogenation–esterification of furfural and acetic acid over bifunctional Pd catalysts for bio-oil upgrading. Bioresour Technol 102(17):8241–8246. doi:10.1016/j.biortech.2011.06.015
5. Nakagawa Y, Tamura M, Tomishige K (2013) Catalytic reduction of biomass-derived furanic compounds with hydrogen. ACS Catal 3 (12):2655–2668. doi:10.1021/cs400616p
6. Triebl C, Nikolakis V, Ierapetritou M (2013) Simulation and economic analysis of 5-hydroxymethylfurfural conversion to 2,5-furandicarboxylic acid. Computers &amp.; Chem Eng 52(0):26–34. doi:10.1016/j.compchemeng.2012.12.005
7. Wettstein SG, Alonso DM, Gürbüz EI, Dumesic JA (2012) A roadmap for conversion of lignocellulosic biomass to chemicals and fuels. Current Opinion in Chemical Engineering 1(3):218–224. doi:10.1016/j.coche.2012.04.002
8. Jiménez-Gómez CP, Cecilia JA, Durán-Martín D, Moreno-Tost R, Santamaría-González J, Mérida-Robles J, Mariscal R, Maireles-Torres P (2016) Gas-phase hydrogenation of furfural to furfuryl alcohol over Cu/ZnO catalysts. J Catal 336:107–115. doi:10.1016/j.jcat.2016.01.012

9. Taylor MJ, Durndell LJ, Isaacs MA, Parlett CMA, Wilson K, Lee AF, Kyriakou G (2016) Highly selective hydrogenation of furfural over supported Pt nanoparticles under mild conditions. Appl Catal B 180:580–585. doi:10.1016/j.apcatb.2015.07.006
10. Yan K, Chen A (2013) Efficient hydrogenation of biomass-derived furfural and levulinic acid on the facilely synthesized noble-metal-free Cu–Cr catalyst. Energy 58:357–363. doi:10.1016/j.energy.2013.05.035
11. Yan K, Wu X, An X, Xie X (2013) Novel preparation of nanocomposite CuO–Cr_2O_3 using CTAB-template method and efficient for hydrogenation of biomass-derived furfural. Functional Mater Lett 6(01):1350007-1350001-1350007–1350007-1350001-1350005. doi:10.1142/S1793604713500070
12. Zhu H, Zhou M, Zeng Z, Xiao G, Xiao R (2014) Selective hydrogenation of furfural to cyclopentanone over Cu–Ni–Al hydrotalcite-based catalysts. Korean J Chem Eng 31(4):593–597. doi:10.1007/s11814-013-0253-y
13. Yuan Q, Zhang D, van Haandel L, Ye F, Xue T, Hensen EJM, Guan Y (2015) Selective liquid phase hydrogenation of furfural to furfuryl alcohol by Ru/Zr-MOFs. J Mol Catal A: Chem 406:58–64. doi:10.1016/j.molcata.2015.05.015
14. Yan K, Chen A (2014) Selective hydrogenation of furfural and levulinic acid to biofuels on the ecofriendly Cu–Fe catalyst. Fuel 115:101–108. doi:10.1016/j.fuel.2013.06.042
15. Sulmonetti TP, Pang SH, Claure MT, Lee S, Cullen DA, Agrawal PK, Jones CW (2016) Vapor phase hydrogenation of furfural over nickel mixed metal oxide catalysts derived from layered double hydroxides. Appl Catal A 517:187–195
16. Halilu A, Ali TH, Atta AY, Sudarsanam P, Bhargava SK, Abd Hamid SB (2016) Highly selective hydrogenation of biomass-derived furfural into furfuryl alcohol using a novel magnetic nanoparticles catalyst. Energy Fuels 30:2216–2226
17. Vargas-Hernández D, Rubio-Caballero JM, Santamaría-González J, Moreno-Tost R, Mérida-Robles JM, Pérez-Cruz MA, Jiménez-López A, Hernández-Huesca R, Maireles-Torres P (2014) Furfuryl alcohol from furfural hydrogenation over copper supported on SBA-15 silica catalysts. J Mol Catal A: Chem 383–384:106–113. doi:10.1016/j.molcata.2013.11.034
18. Manikandan M, Venugopal AK, Nagpure AS, Chilukuri S, Raja T (2016) Promotional effect of Fe on the performance of supported Cu catalyst for ambient pressure hydrogenation of furfural. RSC Adv 6 (5):3888–3898. doi:10.1039/c5ra24742j
19. Sharma RV, Das U, Sammynaiken R, Dalai AK (2013) Liquid phase chemo-selective catalytic hydrogenation of furfural to furfuryl alcohol. Appl Catal A 454:127–136. doi:10.1016/j.apcata.2012.12.010
20. Villaverde MM, Garetto TF, Marchi AJ (2015) Liquid-phase transfer hydrogenation of furfural to furfuryl alcohol on Cu–Mg–Al catalysts. Catal Commun 58:6–10. doi:10.1016/j.catcom.2014.08.021
21. Li J, Liu J-l, Zhou H-j, Fu Y (2016) Catalytic transfer hydrogenation of furfural to furfuryl alcohol over nitrogen-doped carbon-supported iron catalysts. Chem Sus Chem 9(11):1339–1347. doi:10.1002/cssc.201600089
22. Nagaraja BM, Padmasri AH, David Raju B, Rama Rao KS (2007) Vapor phase selective hydrogenation of furfural to furfuryl alcohol over Cu–MgO coprecipitated catalysts. J Mol Catal A 265(1–2):90–97. doi:10.1016/j.molcata.2006.09.037
23. Li M, Hao Y, Cárdenas-Lizana F, Keane MA (2015) Selective production of furfuryl alcohol via gas phase hydrogenation of furfural over Au/Al_2O_3. Catal Commun 69:119–122. doi:10.1016/j.catcom.2015.06.007
24. Xu Y, Qiu S, Long J, Wang C, Chang J, Tan J, Liu Q, Ma L, Wang T, Zhang Q (2015) In situ hydrogenation of furfural with additives over a raney Ni catalyst. RSC Adv 5(111):91190–91195. doi:10.1039/C5RA12844G
25. Yuan Q, Zhang D, van Haandel L, Ye FX, T., Hensen EJM, Guan Y (2015) Selective liquid phase hydrogenation of furfural to furfuryl alcohol by Ru/Zr-MOFs. J Mol Catal A 406:58–64
26. Taylor MJ, Durndell LJ, Isaacs MA, Parlett CMA, Wilson K, Lee AF, Kyriakou G (2016) Highly selective hydrogenation of furfural over supported Ptnanoparticles under mild conditions. Appl Catal, B 180:580–585
27. Kijeński J, Winiarek P, Paryjczak T, Lewicki A, Mikołajska A (2002) Platinum deposited on monolayer supports in selective hydrogenation of furfural to furfuryl alcohol. Appl Catal A 233(1–2):171–182. doi:10.1016/S0926-860X(02)00140-0
28. Nagaraja BM, Padmasri AH, Raju BD, Rama Rao KS (2011) Production of hydrogen through the coupling of dehydrogenation and hydrogenation for the synthesis of cyclohexanone and furfuryl alcohol over different promoters supported on Cu–MgO catalysts. Int J Hydrogen Energy 36(5):3417–3425. doi:10.1016/j.ijhydene.2010.12.013
29. Nakagawa Y, Takada K, Tamura M, Tomishige K (2014) Total hydrogenation of furfural and 5-hydroxymethylfurfural over supported Pd–Ir Alloy catalyst. ACS Catal 4(8):2718–2726
30. Lesiak M, Binczarski M, Karski S, Maniukiewicz W, Rogowski J, Szubiakiewicz E, Berlowska J, Dziugan P, Witońska I (2014) Hydrogenation of furfural over Pd–Cu/Al_2O_3 catalysts. The role of interaction between palladium and copper on determining catalytic properties. J Mol Catal A: Chem 395:337–348. doi:10.1016/j.molcata.2014.08.041
31. An K, Musselwhite N, Kennedy G, Pushkarev VV, Robert Baker L, Somorjai GA (2013) Preparation of mesoporous oxides and their support effects on Pt nanoparticle catalysts in catalytic hydrogenation of furfural. J Colloid Interface Sci 392:122–128. doi:10.1016/j.jcis.2012.10.029
32. Aldosari OF, Iqbal S, Miedziak PJ, Brett GL, Jones DR, Liu X, Edwards JK, Morgan DJ, Knight DK, Hutchings GJ (2016) Pd–Ru/TiO_2 catalyst–an active and selective catalyst for furfural hydrogenation. Catal Sci Technol 6 (1):234–242. doi:10.1039/C5CY01650A
33. Nagaraja BM, Kumar VS, Shasikala V, Padmasri AH, Sreedhar B, Raju BD, Rao KS (2003) A highly efficient Cu/MgO catalyst for vapour phase hydrogenation of furfural to furfuryl alcohol. Catal Commn 4 (6):287–293. doi:10.1016/S1566-7367(03)00060-8
34. Cui H, Wu X, Chen Y, Zhang J, Boughton RI (2015) Influence of copper doping on chlorine adsorption and antibacterial behavior of MgO prepared by co-precipitation method. Mater Res Bull 61:511–518. doi:10.1016/j.materresbull.2014.10.067
35. Estrup AJ (2015) Selective hydrogenation of furfural to furfuyl alcohol over copper magnesium oxide. MSc, University of Maine
36. Liu H, Hu Q, Fan G, Yang L, Li F (2015) Surface synergistic effect in well-dispersed Cu/MgO catalysts for highly efficient vapor-phase hydrogenation of carbonyl compounds. Catal Sci Technol 5(8):3960–3969. doi:10.1039/c5cy00437c
37. Rao R, Dandekar A, Baker RTK, Vannice MA (1997) Properties of copper chromite catalysts in hydrogenation reactions. J Catal 171(2):406–419. doi:10.1006/jcat.1997.1832
38. Deutsch KL, Shanks BH (2012) Active species of copper chromite catalyst in C–O hydrogenolysis of 5-methylfurfuryl alcohol. J Catal 285(1):235–241. doi:10.1016/j.jcat.2011.09.030
39. Seo G, Chon H (1981) Hydrogenation of furfural over copper-containing catalysts. J Catal 67(2):424–429
40. Wu J, Shena Y, Liu C, Wang H, Geng C, Zhang Z (2005) Vapor phase hydrogenation of furfural to furfuryl alcohol over environmentally friendly Cu–Ca/SiO_2 catalyst. Catal Commun 6 (9):633–637. doi:10.1016/j.catcom.2005.06.009
41. Reddy BM, Reddy GK, Rao KN, Khan A, Ganesh I (2007) Silica supported transition metal-based bimetallic catalysts for vapour

phase selective hydrogenation of furfuraldehyde. J Mol Catal A: Chem 265(1–2):276–282. doi:10.1016/j.molcata.2006.10.034
42. Pozan GS, Boz I (2006) Citronellol dehydrogenation over copper-magnesium oxide catalyst. Indian J Chem Technol 13(5):488–492
43. Mallik S, Dash SS, Parida KM, Mohapatra BK (2006) Synthesis, characterization, and catalytic activity of phosphomolybdic acid supported on hydrous zirconia. J Colloid Interface Sci 300(1):237–243. doi:10.1016/j.jcis.2006.03.047
44. Liu X, Liu J, Chang Z, Sun X, Li Y (2011) Crystal plane effect of Fe_2O_3 with various morphologies on CO catalytic oxidation. Catal Commun 12(6):530–534. doi:10.1016/j.catcom.2010.11.016
45. Zhang H, Shao S, Xiao R, Shen D, Zeng J (2014) Characterization of coke deposition in the catalytic fast pyrolysis of biomass derivates. Energy Fuels 28(1):52–57. doi:10.1021/ef401458y
46. Hassan F (2011) Heterogeneous catalysis in supercritical fluids: the enhancement of catalytic stability to coking. PhD Dissertation, University of Birmingham.